


Disorder-Induced Anomalous Mobility Enhancement in Confined GeometriesDan Shafir^{*} and Stanislav Burov[†]*Physics Department, Bar-Ilan University, Ramat Gan 5290002, Israel* (Received 14 March 2024; accepted 14 June 2024; published 19 July 2024)

Strong, scale-free disorder disrupts typical transport properties like the Stokes-Einstein relation and linear response, leading to anomalous diffusion observed in amorphous materials, glasses, living cells, and other systems. Our study reveals that the combination of scale-free quenched disorder and geometrical constraints induces unconventional single-particle mobility behavior. Specifically, in a two-dimensional channel with width w , under external drive, tighter geometrical constraints (smaller w) enhance mobility. We derive an explicit form of the response to an external force by utilizing the double-subordination approach for the quenched trap model. The observed mobility enhancement occurs in the low-temperature regime where the distribution of localization times is scale-free.

DOI: [10.1103/PhysRevLett.133.037101](https://doi.org/10.1103/PhysRevLett.133.037101)

Transport in disordered and amorphous materials has attracted vast attention for many decades [1–10]. The study of systems' response to external forces, particularly with an aim to optimize transport, constitutes an imperative focus of research [11]. The external force can be a result of an electric field pulling on an electron through a conductor [12–14] or a pressure gradient pushing on a molecule diffusing in a channel [15–18]. The classical depiction of such dynamics is Drude's model of current flow in a metal [19]. It describes, through the application of kinetic theory, the diffusion of electrons by repeated encounters with immobile hard scatterers (such as ions or impurities). When an external electric field is applied, the charge carriers experience a net drift velocity related to the mean free path between scattering events. The resulting picture is that the response to the external force, i.e., carrier mobility, is an intrinsic property of the medium. Therefore, for transport in restricted geometry, like a channel, the expectation is that the mobility will be independent of channel width (or cross section) or sometimes will increase with channel width due to the availability of new pathways. In this work, we explore the mobility properties of transport inside a channel with the presence of strong and quenched disorder. Specifically, we aim to demonstrate that quenched and strong disorder can redefine our understanding of the dependence of mobility on geometry.

Experiments in amorphous materials [20–24] have shown that a packet of charge carriers does not propagate in a Gaussian manner and instead exhibits a dispersion of carrier transit times. Scher and Montroll [5,25] termed this phenomenon anomalous transport and suggested that carriers are affected by deep traps or local areas of arrest. When the duration τ of such events follows a power-law distribution, $\sim\tau^{-1-\alpha}$ with $0 < \alpha < 1$, the transport is

subdiffusive [3]; i.e., the mean squared displacement is not proportional to time t but grows sublinearly $\sim t^\alpha$. Subdiffusion was observed in amorphous materials [20–28], biological cells [6,8,29–33], granular materials [10,34,35], non-Newtonian fluids [36], and other systems [37–39]. These power-law distributed waiting times ($\sim\tau^{-(1+\alpha)}$), as detected in various systems [9,36,40–42], can appear naturally due to the exponential distribution of the depths of energetic wells that give rise to the regions of local arrest. The strong disorder ($0 < \alpha < 1$) results in a diverging mean trapping time that disrupts regular diffusive properties and leads to aging, weak ergodicity breaking, and non-self-averaging [43–48]. Most theoretical studies address the annealed version of the strong disorder. Namely, the waiting times in the trapping regions are uncorrelated, and each time the particle returns to the same arrest region, it is localized for a different time. Such framework was termed the continuous time random walk (CTRW) [3,6,25,49], a very popular model of anomalous transport. The quenched version with a strong disorder, termed the quenched trap model (QTM), treats the trapping times during revisits of the arrest region as correlated. For the QTM regular techniques and Stokes-Einstein-Smoluchowski theory do not apply due to strong correlations and memory effects [3,50,51]. Scaling arguments and renormalization group approach [3,52,53] among other works [54–58] suggest that, for dimensions $d > 2$, QTM behaves qualitatively as CTRW in the subdiffusion regime. But big differences can be witnessed, as we show.

In this work, we explore the effects of a strong quenched disorder on particle mobility under the geometrical constraint of a channel with width w . By utilizing the recently developed double-subordination technique [58–62], we obtain an analytical expression for the mobility and its dependence on the external driving force f , temperature T , and width w . For low temperatures, we find that the mobility is a decreasing function of w . Namely, the response to an external drive weakens as the channel cross

^{*}Contact author: dansh5d@gmail.com[†]Contact author: stasbur@gmail.com

section grows. Such a counterintuitive enhancement with decreasing w appears only when the disorder is quenched and strong. When one of these requirements is omitted, the mobility is independent of the channel width.

The quenched trap model—The physical picture behind QTM is a thermally activated particle jumping between energetic traps. When a particle is in a trap, the average escape time τ is provided by the Arrhenius law $\tau \propto \exp(E_{\mathbf{r}}/T)$, where $E_{\mathbf{r}} > 0$ is the depth of trap at position \mathbf{r} and T is the temperature. When the distribution of the energetic traps $E_{\mathbf{r}}$ is exponential, $\phi(E_{\mathbf{r}}) = \exp(-E_{\mathbf{r}}/T_g)/T_g$, where T_g is the temperature of the glass transition, the distribution of the average escape time is [3]

$$\psi(\tau_{\mathbf{r}}) \sim \tau_{\mathbf{r}}^{-1-(T/T_g)} A / |\Gamma(-T/T_g)|, \quad (1)$$

$A = |\Gamma(-T/T_g)|T/T_g$, and $\Gamma(\dots)$ is the Gamma function. For $T < T_g$, the slow power-law decay of $\psi(\tau)$ leads to a diverging mean escape time, when averaged over disorder. In the following, we set $\alpha = T/T_g$ and focus on the glassy regime $0 < \alpha < 1$, where QTM exhibits aging and non-self-averaging behavior [50,51,53]. The average escape times $\tau_{\mathbf{r}}$ serve in QTM as the waiting times. Each time the particle visits position \mathbf{r} , it spends there exactly the same time $\tau_{\mathbf{r}}$; hence, the disorder is quenched. In [47], no difference was found between setting quenched waiting times or setting quenched average waiting times. The quenched variables $\{\tau_{\mathbf{r}}\}$ are positive, independent, identically distributed (i.i.d.) random variables with probability density function (PDF) provided by Eq. (1). We consider the spatial process between different positions \mathbf{r} as a random hop process on a two-dimensional square lattice with lattice spacing a taken to be 1 (a.u.). At time $t = 0$, the particle starts at $\mathbf{r} = 0$ and stays at this position for the period τ_0 before jumping to some random site \mathbf{r}' , where it waits for the period $\tau_{\mathbf{r}'}$, and then the random jump + waiting period procedure continues. The probability of transition (jump) from \mathbf{r} to \mathbf{r}' is provided by $p(\mathbf{r}'; \mathbf{r})$. We assume that the lattice is translationally invariant in space; i.e., $p(\mathbf{r}'; \mathbf{r})$ is a function of $\mathbf{r}' - \mathbf{r}$: $p(\mathbf{r}' - \mathbf{r})$. The disorder averaged positional PDF of finding the particle at position \mathbf{r} at time t , $\langle P(\mathbf{r}, t) \rangle$ ($\langle \dots \rangle$ represents the averaging over disorder) is found by utilizing the double-subordination technique [59,60] that we briefly describe below.

The diffusion front—The effect of correlations imposed by quenched disorder is appreciated when the measurement time t is written in terms of the local waiting times $\tau_{\mathbf{r}}$. Namely, $t = \sum_{\mathbf{r}} n_{\mathbf{r}} \tau_{\mathbf{r}}$, where $n_{\mathbf{r}}$ is the number of visits to \mathbf{r} up to time t . Although all the different $\tau_{\mathbf{r}}$ are i.i.d., the $\{n_{\mathbf{r}}\}$ are correlated, like in our case of nearest-neighbor hopping on a lattice where $n_{\mathbf{r}}$ is very similar to the nearest-neighbor $n_{\mathbf{r}'}$. By fixing the values of $\{n_{\mathbf{r}}\}$ and averaging over $\{\tau_{\mathbf{r}}\}$ (disorder averaging), the $t \rightarrow u$ Laplace transform is $\langle e^{-ut} \rangle \sim e^{-AS_{\alpha}u^{\alpha}}$, where

$$S_{\alpha} = \sum_{\mathbf{r}} (n_{\mathbf{r}})^{\alpha}. \quad (2)$$

The Laplace transform of the one-sided Lévy distribution $l_{\alpha,A,1}(\eta)$ is $\sim e^{-Au^{\alpha}}$, which is also the small u limit of the Laplace transform of a single $\tau_{\mathbf{r}}$. Therefore, in the long time limit ($t \rightarrow \infty$), $t \sim S_{\alpha}^{1/\alpha} \eta$, where η is a random variable distributed according to $l_{\alpha,A,1}(\eta)$. This connection between t , η , and fixed S_{α} allows one to obtain the PDF of S_{α} for fixed t , $\mathcal{N}_t(S_{\alpha})$, by changing variables from $\eta = t/S_{\alpha}^{1/\alpha}$ to $S_{\alpha} = (t/\eta)^{\alpha}$. Therefore, $\mathcal{N}_t(S_{\alpha}) \sim (t/\alpha)(S_{\alpha})^{-1/\alpha-1} l_{\alpha,A,1}[t/(S_{\alpha})^{1/\alpha}]$. The explicit form of $\mathcal{N}_t(S_{\alpha})$ allows performing the first what is commonly called subordination [63] and expresses the disorder averaged $\langle P(\mathbf{r}, t) \rangle$ by using S_{α} as the local time of the process. Namely, for the conditional probability $P_{S_{\alpha}}(\mathbf{r})$ of finding the particle at position \mathbf{r} for a given S_{α} (i.e., at “time” S_{α}), the law of total probability yields

$$\langle P(\mathbf{r}, t) \rangle = \sum_{S_{\alpha}} P_{S_{\alpha}}(\mathbf{r}) \mathcal{N}_t(S_{\alpha}). \quad (3)$$

The second subordination is applied to $P_{S_{\alpha}}(\mathbf{r})$. We use the number of jumps, N , to represent $P_{S_{\alpha}}(\mathbf{r})$ in terms of $W_N(\mathbf{r})$, the probability to find the particle at \mathbf{r} after N jumps, and $\mathcal{G}_{S_{\alpha},\mathbf{r}}(N)$, the probability of different values of N for a prescribed S_{α} and \mathbf{r} . The law of total probability yields $P_{S_{\alpha}}(\mathbf{r}) = \sum_{N=0}^{\infty} W_N(\mathbf{r}) \mathcal{G}_{S_{\alpha},\mathbf{r}}(N)$, and then according to Eq. (3)

$$\langle P(\mathbf{r}, t) \rangle = \sum_{S_{\alpha}} \sum_{N=0}^{\infty} W_N(\mathbf{r}) \mathcal{G}_{S_{\alpha},\mathbf{r}}(N, \mathbf{r}) \mathcal{N}_t(S_{\alpha}). \quad (4)$$

When $t \rightarrow \infty$, also $S_{\alpha} \rightarrow \infty$, and the PDF $\mathcal{G}_{S_{\alpha}}(N, \mathbf{r})$ converges to $\delta(S_{\alpha} - \Lambda N)$ (see Ref. [58]), as long as the probability of eventual return to the origin Q_0 is less than 1. The constant Λ depends on Q_0 and is provided by

$$\Lambda = [(1 - Q_0)^2 / Q_0] Li_{-\alpha}(Q_0), \quad (5)$$

where $Li_{\alpha}(b) = \sum_{j=1}^{\infty} b^j / j^{\alpha}$ is the polylogarithm function [64]. Q_0 is computed when the spatial process is treated as a function of N and will be explicitly found in what follows. Therefore, for QTM where the spatial process is defined solely by the jump probabilities $p(\mathbf{r}' - \mathbf{r})$, Eq. (4) yields

$$\langle P(\mathbf{r}, t) \rangle \sim \sum_N W_N(\mathbf{r}) \frac{t/\Lambda^{1/\alpha}}{\alpha N^{(1/\alpha)-1}} l_{\alpha,A,1}\left(\frac{t/\Lambda^{1/\alpha}}{N^{1/\alpha}}\right). \quad (6)$$

Equation (6), first obtained in [58], presents the disorder averaged propagator of QTM in terms of the spatial process on a lattice as a function of N and a transformation from N to t . Two points are in place: (I) The distribution $W_N(\mathbf{r})$ is defined by the jump probabilities $p(\mathbf{r}' - \mathbf{r})$ and found by the standard techniques for a random walk on a lattice [65]. (II) For $\Lambda = 1$, Eq. (6) displays the propagator for the annealed version of the disorder (CTRW) [3]. Therefore, Λ quantifies

the difference between quenched and annealed disorder as a function of Q_0 [Eq. (5)] which depends on the geometry (type of lattice, dimensions, etc.) and any external forces present in the system. Below, we utilize Eq. (6) and compute the response to external constant force F acting on a single particle in a two-dimensional channel of width w . For this purpose, we first compute the average position along the longitudinal axis of the channel \hat{x} .

The average displacement—The motion occurs on a lattice in a two-dimensional channel and is unrestricted in the \hat{x} direction. The width of the channel, in the \hat{y} direction, is w , which is also the number of sites across \hat{y} (the lattice spacing is $a = 1$). Because of the translational invariance of the spatial process and transition probabilities $p(\mathbf{r} - \mathbf{r}')$, we use periodic boundary conditions for \hat{y} . The case of reflecting boundary conditions will be addressed below. The strength of the force f , applied only along \hat{x} , is characterized by the dimensionless parameter $F = af/T$, where k_B is set to 1. The transition probabilities $p(\mathbf{r} - \mathbf{r}')$ allow transitions only to the nearest neighbors on the square lattice. Namely, p_{\rightarrow} (p_{\leftarrow}) is the probability for a single jump to the right (left) along \hat{x} , and p_{\uparrow} (p_{\downarrow}) is the probability for a single jump up (down) along \hat{y} . The detailed balance condition dictates that $p_{\rightarrow}/p_{\leftarrow} = e^F$ and $p_{\uparrow}/p_{\downarrow} = 1$. Therefore, due to the normalization condition $p_{\uparrow} + p_{\downarrow} + p_{\leftarrow} + p_{\rightarrow} = 1$, we obtain that $p_{\rightarrow} = Be^{F/2}$, $p_{\leftarrow} = Be^{-F/2}$, and $p_{\uparrow} = p_{\downarrow} = B = 1/[2 \cosh(F/2) + 2]$. We are interested in the mean position $\langle x(t) \rangle = \sum_{\mathbf{r}} x \langle P(\mathbf{r}, t) \rangle$. After one single jump, the average displacement along \hat{x} is $p_{\rightarrow} - p_{\leftarrow} = \tanh(F/4)$; therefore, after N jumps, the average displacement is $\sum_{\mathbf{r}} x W_N(\mathbf{r}) = N \tanh(F/4)$. Then according to Eq. (6) $\langle x(t) \rangle = \sum_N N \tanh(F/4) \{Nt/[\alpha(\Lambda N)^{1/\alpha}]\} l_{\alpha,A,1}(t/(\Lambda N)^{1/\alpha})$. We take the limit $t \rightarrow \infty$, replace the summation by integration [3], and use the relation $\int_0^\infty y^q l_{\alpha,A,1}(y) dy = A^{q/\alpha} \Gamma(1 - q/\alpha) / \Gamma(1 - q)$ for $q/\alpha < 1$ [66] to obtain the average displacement in \hat{x} :

$$\langle x(t) \rangle \sim \frac{\tanh(F/4)}{A\Gamma[1 + \alpha]} \frac{Q_0}{(1 - Q_0)^2 \text{Li}_{-\alpha}(Q_0)} t^\alpha. \quad (7)$$

Equation (7) shows that the average displacement is anomalous in time $\sim t^\alpha$. Such departure from the Einstein relation that predicts a linear dependence on time is a direct consequence of diverging mean waiting times and for the annealed disorder was termed as the generalized Einstein relation [67]. To finalize the calculation of $\langle x(t) \rangle$, we find the explicit form of Q_0 .

The return probability Q_0 is computed in terms of $f_N(\mathbf{0})$, the first return probability to the origin after N steps. Namely, $Q_0 = \sum_{N=0}^\infty f_N(\mathbf{0})$. The probability $f_N(\mathbf{0})$ determines the probability $W_N(\mathbf{0})$, since, according to the renewal equation [65], $W_N(\mathbf{0}) = \delta_{N,0} + \sum_{i=1}^N f_i(\mathbf{0}) W_{N-i}(\mathbf{0})$, which yields for the generating function of the first

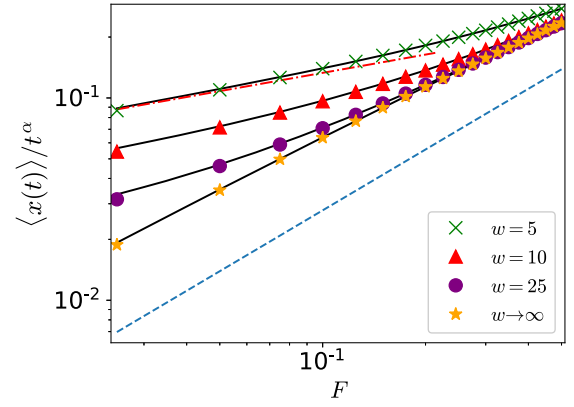


FIG. 1. The average displacement in the direction of F . $\langle x(t) \rangle$ is growing as channel width w is reduced. Solid lines display the theoretical prediction [Eq. (7)]. The red dash-dotted line is the approximation for small F [Eq. (9)]. Symbols are simulation results averaged over 3×10^6 trajectories, $\alpha = 0.3$, $A = 1$, and $t = 10^{14}$ (a.u.). The blue dashed line presents the equivalent annealed disorder (CTRW) system.

return probability $\tilde{f}_z(\mathbf{0}) = \sum_{N=0}^\infty f_N(\mathbf{0}) z^N$ the result $\tilde{f}_z(\mathbf{0}) = 1 - 1/\tilde{W}_z(\mathbf{0})$, where $\tilde{W}_z(\mathbf{0}) = \sum_{N=0}^\infty W_N(\mathbf{0}) z^N$. By noting that $Q_0 = \tilde{f}_1(\mathbf{0})$, the connection between Q_0 and $W_N(\mathbf{0})$ is finally established [65], namely, $Q_0 = 1 - 1/\tilde{W}_{z=1}(\mathbf{0})$. Since $W_N(\mathbf{r})$ is a convolution of N random variables, i.e., steps, its Fourier transform is the N th power of the single-step characteristic function $\lambda(\mathbf{k}) = e^{ik_x} p_{\rightarrow} + e^{-ik_x} p_{\leftarrow} + e^{ik_y} p_{\uparrow} + e^{-ik_y} p_{\downarrow}$ and, therefore, $\tilde{W}_{z=1}(\mathbf{0}) = (1/4\pi^2) \int_{-\pi}^{\pi} \int_{-\pi}^{\pi} \{1/[1 - \lambda(\mathbf{k})]\} dk_x dk_y$. In Supplemental Material [68], we compute this integral and show that

$$Q_0 = 1 - \frac{w/[1 + \cosh(F/2)]}{\sum_{m=0}^{w-1} 1/\sqrt{[1 + \cosh(F/2) - \cos(2\pi m/w)]^2 - 1}}. \quad (8)$$

When $w \rightarrow \infty$, the result in Eq. (8) converges to the known result [5] for an unbounded two-dimensional square lattice $\lim_{w \rightarrow \infty} Q_0 = 1 - 1/[(2/\pi) \mathbf{K}(4/[1 + \cosh(F/2)]^2)]$, where $\mathbf{K}(k) = \int_0^{\pi/2} d\gamma (1 - k \sin^2 \gamma)^{-1/2}$ is the complete elliptic integral of the first kind [64].

Equations (7) and (8) present $\langle x(t) \rangle$ in a channel of width w under a constant force F , in the limit of large t . For small forces, Eq. (7) yields (see Supplemental Material [68])

$$\langle x(t) \rangle \sim \frac{w^{\alpha-1}}{A\Gamma^2[1 + \alpha]} \left(\frac{F}{4}\right)^\alpha t^\alpha, \quad (9)$$

while $4/F \gg w/\sqrt{2}$ and w is an integer ≥ 1 . Our main result is immediately apparent from Eq. (9): $\langle x(t) \rangle$ unexpectedly decays with growing channel width w . The dependence is $w^{\alpha-1}$, meaning the motion is faster for narrow channels than for wide channels. In Fig. 1, we

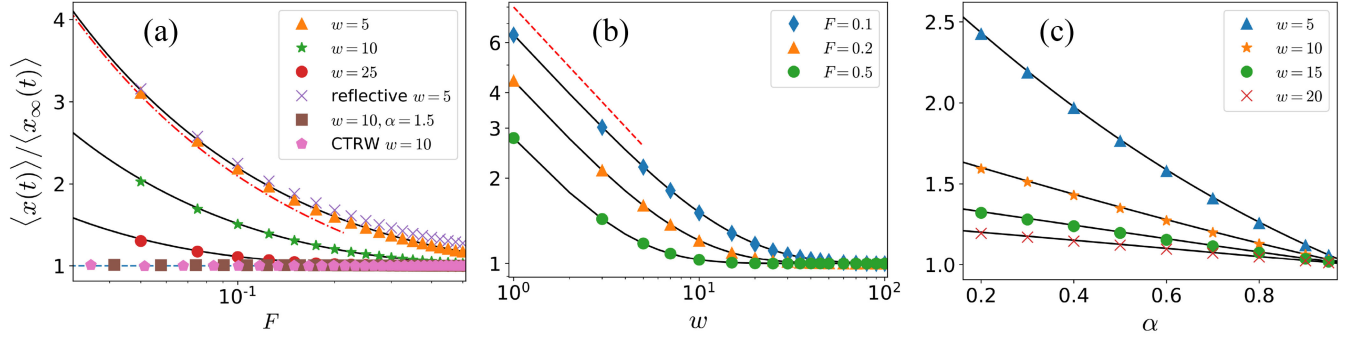


FIG. 2. Enhancement of mobility in a channel of width w [$\langle x(t) \rangle$] with respect to mobility in unrestricted 2D geometry [$\langle x_\infty(t) \rangle$], as a function of external force F (a), width w (b), and $\alpha = T/T_g$ (c). In all panels, Eq. (7) [combined with Eq. (8)] is displayed by solid black lines, and the symbols are the results of numerical simulations. (a) The red dash-dotted line is the small- F expansion, while the leading term is provided by Eq. (10) (see Supplemental Material [68] for the full expression). \times presents simulation results for reflective boundary conditions and $w = 5$ that almost follows the corresponding case with periodic boundary conditions \triangle . The blue dashed line represents the case when no enhancement was detected: for annealed disorder (CTRW) and QTM with a finite average dwell times ($\alpha > 1$). For all cases $t = 10^{14}$ (a.u.) and except \square , $\alpha = 0.3$. (b) The red dashed line indicates the $w^{\alpha-1}$ scaling, $\alpha = 0.3$, and $t = 10^{14}$ (a.u.). (c) $F = 0.1$ and $t^\alpha = 4.2$ (a.u.). For all panels, $A = 1$.

present an excellent agreement between Eq. (8) and numerical simulations. For small F , the dependence is simplified to $\sim F^\alpha$. Namely, the strong disorder and its quenched nature that impose prolonged correlations make the usual assumption of linear response inapplicable in the quasi 2D, as was found previously for 1D QTM [3,58,59,74]. We note that for the case of strong annealed disorder (CTRW) the dependence on F (when $F \rightarrow 0$) is linear [59] (see the dashed line in Fig. 1).

To emphasize the mobility enhancement due to the channel width constraint, we calculate (see Supplemental Material [68]) the ratio of the $\langle x(t) \rangle$ for a given w and the average displacement for unrestricted 2D motion, $\langle x_\infty(t) \rangle$, i.e., $w \rightarrow \infty$. For $F \rightarrow 0$, we obtain

$$\langle x(t) \rangle / \langle x_\infty(t) \rangle \sim [(w/4\pi)F \ln(128/F^2)]^{\alpha-1}, \quad (10)$$

implying that imposing a geometrical constraint enhances the transport, and the stronger the constraint (narrower channel), the larger the enhancement. Note that the logarithmic term in F enters Eq. (10) due to the critical properties of Q_0 in unrestricted 2D (see Ref. [59] and Supplemental Material [68]). In Fig. 2, we present the excellent agreement between the analytical results for $\langle x(t) \rangle / \langle x_\infty(t) \rangle$ and numerical simulations when explored as a function of F , w , and α . The enhancement associated with geometrical restriction repeats itself in all the presented cases and is preserved for smaller times (see Supplemental Material [68]). Figure 2(a) shows that the effect disappears: $\langle x(t) \rangle / \langle x_\infty(t) \rangle = 1$ when the disorder is not strong ($\alpha > 1$) or if the disorder is not quenched.

In our derivation, we assumed periodic boundary conditions. In Fig. 2(a), we show that reflecting conditions produce similar behavior. See Supplemental Material [68] for additional details.

Equation (9) summarizes the unconventional effect of strong and quenched disorder. The regular expectation for $\langle x(t) \rangle$ is $\langle x(t) \rangle = \mu Ft$, where μ is the mobility. Strong disorder modifies the temporal dependence and the regular Einstein relation. Quenchness breaks linear response and introduces the nonlinear dependence on F , and here we have shown that the properties of the mobility μ are counterintuitive. First of all, the mobility μ for QTM is anomalous since it cannot be defined as $\langle x(t) \rangle / tF$ but rather as $\mu = \langle x(t) \rangle / t^\alpha F^\alpha$. From Eq. (9), $\mu = w^{\alpha-1} / 4^\alpha A \Gamma^2[\alpha + 1]$ while $\alpha = T/T_g < 1$. The mobility is enhanced as the channel width w decreases. While the expectation is that additional pathways, which start to appear with relaxed geometrical constraints, will lead to a speedup of the transport [75], we observe an opposite behavior. In the presence of strong and quenched disorder, stricter geometrical constraints improve mobility.

Mathematical reasons for such counterintuitive enhancement are rooted in the properties of the local time S_α , transformation constraint Λ , and geometrical dependence of Q_0 . The intuition behind the found effect is based on what is known as the “big jump principle” [76–78]. When scale-free waiting times [Eq. (1)] are in play, it is not the accumulation of many events but rather a single maximal event that governs the overall behavior. In our case, this dominant event is a single extremely long waiting time that scales as the total measurement time t , during which the particle is immobilized. Naturally, when such a single event is excluded, for example, by replacing the site with a maximal waiting time by significantly shorter τ , it will lead to faster transport [79]. Our results suggest that narrowing the channel width decreases the number of possible sites the particle will sample during transport and effectively modifies this single dominant arrest time. This reduction of the single dominant arrest time means that, on average,

during time t , the particle will be trapped for a shorter time in one single position. The saved time will be used to perform more hops, increasing its average displacement and enhancing mobility. The quenched nature of the disorder is a crucial ingredient for this to work. A further in-depth analysis and experimental research of this phenomenon is warranted. We expect that such enhancement will be useful to optimize transport in a channel media relevant for applications in nanotechnology and nanomedicine [11] and transport in porous media [79]. Our theory will become useful in systems that change significantly slower than the dynamics within them. As this work shows, the quenched nature of the disorder cannot be simply neglected. For example, quenched disorder appears in transport driven by molecular motors on F-actin filament networks [29], neurons in the brain [80], and other active systems [81–83] where the escape times from trapping regions are correlated.

Acknowledgments—This work was supported by the Israel Science Foundation Grant No. 2796/20.

- [1] S. Scott, M. Weiss, C. Selhuber-Unkel, Y.F. Barooji, A. Sabri, J.T. Erler, R. Metzler, and L.B. Oddershede, Extracting, quantifying, and comparing dynamical and biomechanical properties of living matter through single particle tracking, *Phys. Chem. Chem. Phys.* **25**, 1513 (2023).
- [2] T. A. Waigh and N. Korabel, Heterogeneous anomalous transport in cellular and molecular biology, *Rep. Prog. Phys.* **86**, 126601 (2023).
- [3] J.-P. Bouchaud and A. Georges, Anomalous diffusion in disordered media: Statistical mechanisms, models and physical applications, *Phys. Rep.* **195**, 127 (1990).
- [4] R. Metzler and J. Klafter, The random walk's guide to anomalous diffusion: A fractional dynamics approach, *Phys. Rep.* **339**, 1 (2000).
- [5] E. W. Montroll and B. J. West, *On an Enriched Collection of Stochastic Processes* (North-Holland, La Jolla, California, 1979).
- [6] R. Metzler, J.-H. Jeon, A. G. Cherstvy, and E. Barkai, Anomalous diffusion models and their properties: Non-stationarity, non-ergodicity, and ageing at the centenary of single particle tracking, *Phys. Chem. Chem. Phys.* **16**, 24128 (2014).
- [7] E. Barkai, Y. Garini, and R. Metzler, Strange kinetics of single molecules in living cells, *Phys. Today* **65**, No. 8, 29 (2012).
- [8] S. J. Anderson, C. Matsuda, J. Garamella, K. R. Peddireddy, R. M. Robertson-Anderson, and R. McGorty, Filament rigidity vies with mesh size in determining anomalous diffusion in cytoskeleton, *Biomacromolecules* **20**, 4380 (2019).
- [9] E. Yamamoto, T. Akimoto, A. Mitsutake, and R. Metzler, Universal relation between instantaneous diffusivity and radius of gyration of proteins in aqueous solution, *Phys. Rev. Lett.* **126**, 128101 (2021).
- [10] R. Metzler, A. Rajyaguru, and B. Berkowitz, Modelling anomalous diffusion in semi-infinite disordered systems and porous media, *New J. Phys.* **24**, 123004 (2022).
- [11] P. Magaretti, G. Oshanin, and J. Talbot, Special issue on transport in narrow channels, *J. Phys. Condens. Matter* **31**, 270201 (2019).
- [12] S. Kondrat, P. Wu, R. Qiao, and A. A. Kornyshev, Accelerating charging dynamics in subnanometre pores, *Nat. Mater.* **13**, 387 (2014).
- [13] A. A. Lee, S. Kondrat, G. Oshanin, A. A. Kornyshev *et al.*, Charging dynamics of supercapacitors with narrow cylindrical nanopores, *Nanotechnology* **25**, 315401 (2014).
- [14] O. Bénichou, P. Illien, G. Oshanin, A. Sarracino, and R. Voituriez, Tracer diffusion in crowded narrow channels, *J. Phys. Condens. Matter* **30**, 443001 (2018).
- [15] W. E. Uspsal, H. Burak Eral, and P. S. Doyle, Engineering particle trajectories in microfluidic flows using particle shape, *Nat. Commun.* **4**, 2666 (2013).
- [16] A. Sarracino, F. Cecconi, A. Puglisi, and A. Vulpiani, Nonlinear response of inertial tracers in steady laminar flows: Differential and absolute negative mobility, *Phys. Rev. Lett.* **117**, 174501 (2016).
- [17] F. Cecconi, A. Puglisi, A. Sarracino, and A. Vulpiani, Anomalous force-velocity relation of driven inertial tracers in steady laminar flows, *Eur. Phys. J. E* **40**, 1 (2017).
- [18] F. Cecconi, A. Puglisi, A. Sarracino, and A. Vulpiani, Anomalous mobility of a driven active particle in a steady laminar flow, *J. Phys. Condens. Matter* **30**, 264002 (2018).
- [19] N. W. Ashcroft and N. Mermin, *Solid State, Physics* (Holt, Rinehart and Winston, New York, 1976).
- [20] M. Scharfe, Transient photoconductivity in vitreous As_2Se_3 , *Phys. Rev. B* **2**, 5025 (1970).
- [21] D. M. Pai and M. E. Scharfe, Charge transport in films of amorphous arsenic triselenide, *J. Non-Cryst. Solids* **8**, 752 (1972).
- [22] G. Pfister, Pressure-dependent electronic transport in amorphous As_2Se_3 , *Phys. Rev. Lett.* **33**, 1474 (1974).
- [23] J. Mort and A. Lakatos, Steady state and transient photoemission into amorphous insulators, *J. Non-Cryst. Solids* **4**, 117 (1970).
- [24] W. Gill, Drift mobilities in amorphous charge-transfer complexes of trinitrofluorenone and poly-n-vinylcarbazole, *J. Appl. Phys.* **43**, 5033 (1972).
- [25] H. Scher and E. W. Montroll, Anomalous transit-time dispersion in amorphous solids, *Phys. Rev. B* **12**, 2455 (1975).
- [26] Y. Yuan, B. A. Gregg, and M. F. Lawrence, Time-of-flight study of electrical charge mobilities in liquid-crystalline zinc octakis (β -octoxyethyl) porphyrin films, *J. Mater. Res.* **15**, 2494 (2000).
- [27] A. Tyutnev, D. Weiss, V. Saenko, and E. Pozhidaev, About mobility thickness dependence in molecularly doped polymers, *Chem. Phys.* **495**, 16 (2017).
- [28] D. Dunlap, Hopping transport in molecularly doped polymers: On the relation between disorder and a field-dependent mobility, *J. Imaging Sci. Technol.* **40**, 291 (1996).
- [29] M. Scholz, S. Burov, K. L. Weirich, B. J. Scholz, S. A. Tabei, M. L. Gardel, and A. R. Dinner, Cycling state that can lead to glassy dynamics in intracellular transport, *Phys. Rev. X* **6**, 011037 (2016).

- [30] E. Barkai, Y. Garini, and R. Metzler, Strange kinetics of single molecules in living cells, *Phys. Today* **65**, No. 8, 29 (2012).
- [31] V. P. S. Kompella, M. C. Romano, I. Stansfield, and R. L. Mancera, What determines sub-diffusive behavior in crowded protein solutions?, *Biophys. J.* **123**, 134 (2024).
- [32] S. Yu, J. Sheats, P. Cicuta, B. Scavi, M. Cosentino Lagomarsino, and K. D. Dorfman, Subdiffusion of loci and cytoplasmic particles are different in compressed *Escherichia coli* cells, *Comm. Biol.* **1**, 176 (2018).
- [33] A. Sabri, X. Xu, D. Krapf, and M. Weiss, Elucidating the origin of heterogeneous anomalous diffusion in the cytoplasm of mammalian cells, *Phys. Rev. Lett.* **125**, 058101 (2020).
- [34] G. Marty and O. Dauchot, Subdiffusion and cage effect in a sheared granular material, *Phys. Rev. Lett.* **94**, 015701 (2005).
- [35] A. S. Bodrova, Diffusion in multicomponent granular mixtures, *Phys. Rev. E* **109**, 024903 (2024).
- [36] I. Y. Wong, M. L. Gardel, D. R. Reichman, E. R. Weeks, M. T. Valentine, A. R. Bausch, and D. A. Weitz, Anomalous diffusion probes microstructure dynamics of entangled *f*-actin networks, *Phys. Rev. Lett.* **92**, 178101 (2004).
- [37] P. G. Meyer and R. Metzler, Time scales in the dynamics of political opinions and the voter model, *New J. Phys.* **26**, 023040 (2024).
- [38] S. A. McKinley, L. Yao, and M. G. Forest, Transient anomalous diffusion of tracer particles in soft matter, *J. Rheol.* **53**, 1487 (2009).
- [39] M. Paoluzzi, D. Levis, and I. Pagonabarraga, From flocking to glassiness in dense disordered polar active matter, *Commun. Phys.* **7**, 57 (2024).
- [40] S. A. Tabei, S. Burov, H. Y. Kim, A. Kuznetsov, T. Huynh, J. Jureller, L. H. Philipson, A. R. Dinner, and N. F. Scherer, Intracellular transport of insulin granules is a subordinated random walk, *Proc. Natl. Acad. Sci. U.S.A.* **110**, 4911 (2013).
- [41] O. Vilks, Y. Orchan, M. Charter, N. Ganot, S. Toledo, R. Nathan, and M. Assaf, Ergodicity breaking in area-restricted search of avian predators, *Phys. Rev. X* **12**, 031005 (2022).
- [42] O. Vilks, E. Aghion, R. Nathan, S. Toledo, R. Metzler, and M. Assaf, Classification of anomalous diffusion in animal movement data using power spectral analysis, *J. Phys. A* **55**, 334004 (2022).
- [43] J.-P. Bouchaud, Weak ergodicity breaking and aging in disordered systems, *J. Phys. I* **2**, 1705 (1992).
- [44] C. Monthus and J.-P. Bouchaud, Models of traps and glass phenomenology, *J. Phys. A* **29**, 3847 (1996).
- [45] B. Rinn, P. Maass, and J.-P. Bouchaud, Multiple scaling regimes in simple aging models, *Phys. Rev. Lett.* **84**, 5403 (2000).
- [46] B. Rinn, P. Maass, and J.-P. Bouchaud, Hopping in the glass configuration space: Subaging and generalized scaling laws, *Phys. Rev. B* **64**, 104417 (2001).
- [47] E. M. Bertin and J.-P. Bouchaud, Subdiffusion and localization in the one-dimensional trap model, *Phys. Rev. E* **67**, 026128 (2003).
- [48] S. Burov and E. Barkai, Occupation time statistics in the quenched trap model, *Phys. Rev. Lett.* **98**, 250601 (2007).
- [49] O. Hamdi, S. Burov, and E. Barkai, Laplace's first law of errors applied to diffusive motion, *Eur. Phys. J. B* **97**, 67 (2024).
- [50] T. Akimoto, E. Barkai, and K. Saito, Non-self-averaging behaviors and ergodicity in quenched trap models with finite system sizes, *Phys. Rev. E* **97**, 052143 (2018).
- [51] T. Akimoto and K. Saito, Trace of anomalous diffusion in a biased quenched trap model, *Phys. Rev. E* **101**, 042133 (2020).
- [52] J. Machta, Random walks on site disordered lattices, *J. Phys. A* **18**, L531 (1985).
- [53] C. Monthus, Anomalous diffusion, localization, aging, and subaging effects in trap models at very low temperature, *Phys. Rev. E* **68**, 036114 (2003).
- [54] G. Ben Arous, J. Černý, and T. Mountford, Aging in two-dimensional bouchaud's model, *Probab. Theory Related Fields* **134**, 1 (2006).
- [55] G. B. Arous and J. Černý, Scaling limit for trap models on, *Ann. Probab.* **35**, 2356 (2007).
- [56] G. B. Arous, M. Cabezas, J. Černý, and R. Royfman, Randomly trapped random walks, *Ann. Probab.* **43**, 2405 (2015).
- [57] J. Černý and T. Wassmer, Randomly trapped random walks on \mathbb{Z}^d , *Stoch. Proc. Appl.* **125**, 1032 (2015).
- [58] S. Burov, From quenched disorder to continuous time random walk, *Phys. Rev. E* **96**, 050103(R) (2017).
- [59] D. Shafir and S. Burov, The case of the biased quenched trap model in two dimensions with diverging mean dwell times, *J. Stat. Mech.* (2022) 033301.
- [60] S. Burov, The transient case of the quenched trap model, *J. Stat. Mech.* (2020) 073207.
- [61] S. Burov and E. Barkai, Weak subordination breaking for the quenched trap model, *Phys. Rev. E* **86**, 041137 (2012).
- [62] S. Burov and E. Barkai, Time transformation for random walks in the quenched trap model, *Phys. Rev. Lett.* **106**, 140602 (2011).
- [63] J. Klafter and I. M. Sokolov, *First Steps in Random Walks: From Tools to Applications* (Oxford University Press, Oxford, 2011).
- [64] M. Abramowitz, I. A. Stegun, and R. H. Romer, *Handbook of Mathematical Functions with Formulas, Graphs, and Mathematical Tables* (American Association of Physics Teachers, 1988).
- [65] G. H. Weiss, *Aspects and Applications of the Random Walk* (Elsevier Science & Technology, New York, 1994).
- [66] E. Barkai, Fractional Fokker-Planck equation, solution, and application, *Phys. Rev. E* **63**, 046118 (2001).
- [67] E. Barkai and V. N. Fleurov, Generalized Einstein relation: A stochastic modeling approach, *Phys. Rev. E* **58**, 1296 (1998).
- [68] See Supplemental Material at <http://link.aps.org/supplemental/10.1103/PhysRevLett.133.037101> for the in-depth presentation of analytical derivations, which includes Refs. [69–73].
- [69] B. D. Hughes, *Random Walks and Random Environments: Random Walks* (Oxford University Press, New York, 1995), Vol. 1.

- [70] E. W. Montroll and H. Scher, Random walks on lattices. IV. Continuous-time walks and influence of absorbing boundaries, *J. Stat. Phys.* **9**, 101 (1973).
- [71] I. S. Gradshteyn and I. M. Ryzhik, *Table of Integrals, Series, and Products* (Academic Press, New York, 2014).
- [72] M. Brummelhuis and H. Hilhorst, Single-vacancy induced motion of a tracer particle in a two-dimensional lattice gas, *J. Stat. Phys.* **53**, 249 (1988).
- [73] K. F. Riley, M. P. Hobson, and S. J. Bence, *Mathematical Methods for Physics and Engineering* (Cambridge University Press, 1999).
- [74] C. Monthus, Nonlinear response of the trap model in the aging regime: Exact results in the strong-disorder limit, *Phys. Rev. E* **69**, 026103 (2004).
- [75] D. Schwarcz and S. Burov, Self-assembly of two-dimensional, amorphous materials on a liquid substrate, *Phys. Rev. E* **105**, L022601 (2022).
- [76] A. Vezzani, E. Barkai, and R. Burioni, Single-big-jump principle in physical modeling, *Phys. Rev. E* **100**, 012108 (2019).
- [77] A. Vezzani, E. Barkai, and R. Burioni, Rare events in generalized lévy walks and the big jump principle, *Sci. Rep.* **10**, 2732 (2020).
- [78] R. K. Singh and S. Burov, Universal to nonuniversal transition of the statistics of rare events during the spread of random walks, *Phys. Rev. E* **108**, L052102 (2023).
- [79] M. Höll, A. Nissan, B. Berkowitz, and E. Barkai, Controls that expedite first-passage times in disordered systems, *Phys. Rev. E* **108**, 034124 (2023).
- [80] N. Hirokawa, S. Niwa, and Y. Tanaka, Molecular motors in neurons: Transport mechanisms and roles in brain function, development, and disease, *Neuron* **68**, 610 (2010).
- [81] H. Tokuo, S. Komaba, and L. M. Coluccio, In pancreatic β -cells myosin 1b regulates glucose-stimulated insulin secretion by modulating an early step in insulin granule trafficking from the Golgi, *Mol. Biol. Cell* **32**, 1210 (2021).
- [82] D. Vahabli and T. Vicsek, Emergence of synchronised rotations in dense active matter with disorder, *Commun. Phys.* **6**, 56 (2023).
- [83] D. M. Van Roon, G. Volpe, M. M. T. da Gama, and N. A. Araújo, The role of disorder in the motion of chiral active particles in the presence of obstacles, *Soft Matter* **18**, 6899 (2022).